J Ind Microbiol Biotechnol (2012) 39:537–546
DOI 10.1007/s10295-011-1061-1

BIOCATALYSIS

Engineered glucose isomerase from *Streptomyces* sp. SK is resistant to Ca^{2+} inhibition and Co^{2+} independent

Hajer Ben Hlima · Nushin Aghajari · Mamdouh Ben Ali · Richard Haser · Samir Bejar

Received: 9 September 2011 / Accepted: 8 November 2011 / Published online: 4 December 2011
© Society for Industrial Microbiology and Biotechnology 2011

Abstract The role of two amino acid residues linked to the two catalytic histidines His54 and His220 in kinetics and physicochemical properties of the *Streptomyces* sp. SK glucose isomerase (SKGI) was investigated by site-directed mutagenesis and molecular modeling. Two single mutations, F53L and G219D, and a double mutation F53L/G219D was introduced into the *xylA* SKGI gene. The F53L mutation increases the thermostability and the catalytic efficiency and also slightly shifts the optimum pH from 6.5 to 7, but displays a profile being similar to that of the wild-type enzyme concerning the effect of various metal ions. The G219D mutant is resistant to calcium inhibition retaining about 80% of its residual activity in 10 mM Ca^{2+} instead of 10% for the wild-type. This variant is activated by Mn^{2+} ions, but not Co^{2+}, as seen for the wild-type enzyme. It does not require the latter for its thermostability, but has its half-life time displaced from 50 to 20 min at 85°C. The double mutation F53L/G219D restores the thermostability as seen for the wild-type enzyme while maintaining the resistance to the calcium inhibition. Molecular modeling suggests that the increase in thermostability is due to new hydrophobic interactions stabilizing α2 helix and that the resistance to calcium inhibition is a result of narrowing the binding site of catalytic ion.

Keywords *Streptomyces* · Glucose isomerase · Site-directed mutagenesis · Thermostability · Calcium inhibition

H. Ben Hlima · M. Ben Ali · S. Bejar (✉)
Laboratoire de Microorganismes et de Biomolécules, Centre de Biotechnologie de Sfax, Université de Sfax, Route de Sidi Mansour Km 6, B.P 1177, 3018 Sfax, Tunisia
e-mail: samir.bejar@cbs.rnrt.tn

N. Aghajari · R. Haser
Laboratoire de BioCristallographie et Biologie Structurale des Cibles Thérapeutiques, Bases Moléculaires et Structurales des Systèmes Infectieux, UMR 5086–CNRS/Université Lyon 1, Institut de Biologie et Chimie des Protéines, FR3302, 7 Passage du Vercors, 69367 Lyon cedex 07, France

Introduction

Xylose isomerase (XI) (EC 5.3.1.5) plays an essential role in the metabolism of sugars in microorganisms. The enzyme is found in a number of bacteria and catalyzes the isomerization of D-xylose to D-xylulose in vivo. The practical importance of the enzyme stems from its ability to isomerize D-glucose to D-fructose under certain conditions in vitro; therefore, the enzyme is often referred to as glucose isomerase (GI) and utilized in industry for the production of high-fructose corn syrup (HFCS) from corn starch. This process involves several separate enzymatic steps, including liquefaction of corn starch by α-amylase, saccharification by glucoamylase, and isomerization by glucose isomerase [17]. Typically, high temperatures have the advantage of a higher equilibrium concentration of fructose, a faster reaction rate, and a decreased viscosity of the substrate in the product stream [10]. The enzyme is active in dimeric or tetrameric forms and requires Mg^{2+}, Mn^{2+} or Co^{2+} for catalytic activity and thermostability, whereas Ca^{2+} is a strong competitive inhibitor even at low concentrations [4]. The latter ion has a practical importance in the starch bioconversion process, since α-amylases require Ca^{2+} ions for its activity. Thus, it is very important to identify a GI not being inhibited by this ion or an α-amylase, which acts at low calcium concentration. In this context, several studies have been developed concerning

α-amylase [20, 31], but only a few have been done on glucose isomerases. Resistance to Ca^{2+} inhibition allows having the same operational conditions of starch enzymatic saccharification and glucose bioconversion to fructose [4]. This moreover allows a reduction in the process cost by avoiding a Ca^{2+} removal step.

In addition, most of the known GIs require 0.5 to 10 mM Co^{2+} for their thermoactivity and thermostability [35]. Even though Co^{2+} is an essential trace metal for human nutrition, it is toxic at higher levels [12, 32]. The Co^{2+} content of fructose syrups, after the glucose bioconversion step, is about 1 mM [11]. Consequently, and due to human health and pollution problems, fructose syrups must be treated with ion exchange to mainly reduce the cobalt content to acceptable levels [22, 30]. Therefore, it is essential to find a Co^{2+} independent GI to reduce the process cost.

Crystal structures of several D-xylose isomerases have been solved and display a high degree of structural homology: each subunit folds into a main N-terminal domain, with a typical "triose-phosphate isomerase (TIM) barrel" motif with an eight stranded parallel β-sheet surrounded by eight α-helices and a C-terminal helical domain, which forms a large loop. It was also demonstrated that the well-conserved active site contains two metal cations per subunit. The structural metal at site 1 (called M1) is required for substrate binding, whereas the catalytic metal at site 2 (called M2) plays a role in the isomerization [4].

GI isolated from the thermophile *Streptomyces* sp. SK (SKGI) strain encodes a 386-amino-acid protein (42.7 kDa) and shows extensive identities with many other bacterial glucose isomerases. SKGI is a homotetramer having a maximal activity at pH 6.5 and 85°C, which due to its high thermostability and acid-tolerance, is an attractive enzyme for industrial applications [5, 6, 33].

The present work describes the important role of two amino acids, F53 and G219, which are linked to the two catalytic histidines in the SKGI on the SKGI properties. Two single mutants and a double mutant were generated and their effects on kinetics and physicochemical properties of SKGI were studied. The double mutant was significantly less sensitive to Ca^{2+} inhibition and independent of Co^{2+} for its thermoactivity/thermostability.

Materials and methods

Bacterial strains, media, and vectors

Streptomyces sp. SK [33] has been deposited in the Tunisian Culture Collection "CTM" of the Center of Biotechnology of Sfax under the number CTM50547.

Escherichia coli strain DH5α was used as cloning host. For expression, *E. coli* strain BL21 (DE3) (Invitrogen), which contains the structural gene for T7 RNA polymerase under control of the lac promoter, was used. *E. coli* strains were grown in Luria–Bertani medium supplemented, when necessary, with ampicillin (100 μg/ml) and IPTG (16 μg/ml). The plasmid pBSK3 containing the gene encoding wild-type SKGI [33] was used as template for PCR amplification. The plasmid pET-21a (Novagen, USA) including the T7 promoter, was used for the over-expression of the gene encoding native SKGI and its mutants. Plasmids pHB10, pHB14, pHB9, and pHB18 contain the gene encoding native SKGI, F53L, G219D, and F53L/G219D mutant enzymes, respectively.

DNA manipulation and PCR

DNA preparation, endonucleases digestion, and fragments separation by agarose gel electrophoresis were performed as described by Sambrook et al. in 1989 [29]. Restriction endonucleases were purchased from New England Biolabs (MA, USA). PCR was carried out in a Gene Amp PCR System 2,700 thermal cycler (Applied Biosystems, USA). The amplification reaction mixtures (50 μl) contained 2 U of Pfu enzyme (*Pyrococcus furiosis* DNA polymerase) (Appligene), amplification buffer, 20 pg of each primer and 200 ng of DNA template. The cycling parameters were 94°C for 5 min, followed by 40 cycles of 94°C for 30 s, 64°C for 60 s, and 72°C for 120 s. PCR products were purified using an agarose gel extraction kit (Jena Bioscience, Germany).

Construction, over-expression, and cloning of wild-type and mutant genes

SKGI mutants were generated using the coding sequence of the WT gene as template (accession number Y15518), and the mutation was introduced through PCR-based site-directed mutagenesis. Hence, two non-mutagenic external primers (forward (5′-GCCGCCATATGAACTACCAGCC CACC-3′) and reverse (5′-CGTCGAAGCTTGCCGCGG GCG-3′)) and two complementary internal primers containing the desired mutation were designed. The mutagenic primers for the mutation G219D are forward (5′-GTGTCAA CCCCGAGGTG**GAC**CACGAGCAG-3′) and reverse (5′-CTGCTCGTG**GTC**CACCTCGGGGTTGACAC-3′) (bold and underlined nucleotides are the mutation sites). To generate the SKGI F53L mutation, the same external PCR primers as the SKGI G219D were used and the internal one are forward (5′-GCCTACGGAGTGACC**TTG**CACGACG ACGAC-3′) and reverse (5′-GTCGTCGTCGTG**CAA**GGT CACTCCGTAGGC-3′). External PCR primers were also used to amplify the SKGI wild-type gene using pBSK3 as

template. These two primers (forward and reverse), contain the sequence recognized by the two restriction enzymes *Nde*I and *Hind*III (underlined sequences), respectively. Wild-type and mutated genes (1.26 kb) were then purified using the gel band purification kit with a GFX^{TM} column (Amersham Biosciences), double digested with *Nde*I-*Hind*III and ligated into the *Nde*I-*Hind*III linearized pET-21a vector. This construction placed the glucose isomerase gene under control of a T7 promoter, which greatly over-expressed the gene and facilitated the protein purification process, thus generating plasmids pHB10, pHB14 and pHB9 encoding, SKGI, F53L, and G219D mutant genes, respectively. The double mutant F53L/G219D gene was obtained using the same internal primer as the mutant G219D with plasmid pHB14 as template and the plasmid obtained after cloning in pET-21a is named pHB18.

The generated plasmids were transformed into *E. coli* DH5α competent cells and the colonies were grown in LB medium containing ampicillin (100 μg/ml). In order to identify positive colonies, plasmids were extracted using a plasmid extraction kit (Promega, USA), double digested with *Nde*I/*BamH*I followed by agarose gel analysis. The presence of the desired mutations, as well as the absence of other undesirable changes, were confirmed by DNA sequencing using an automated DNA sequencer ABI Prism® 3100-Avant Genetic Analyser from Applied Biosystems (California, USA) using the Big-Dye terminator cycle sequencing kit as recommended by the manufacturer (Amersham Pharmacia Biotech). The isolated plasmids were then used to transform *E. coli* strain BL21 (DE3) competent cells for expression purposes.

Purification of the His6 enzymes

The culture of *E. coli* BL21 (DE3) cells containing the recombinant plasmids were grown at 37°C in LB medium containing 100 μg/ml ampicillin to reach an OD600 nm of 0.3. Then, it was adjusted to 16 μg/ml IPTG and the incubation continued at 37°C for 16 h. Cells were harvested by centrifugation at (7,500 × *g*, 10 min). Pellets were crushed with the same weight of powder aluminia (aluminum oxide Type A-5, Sigma A2039; Sigma-Aldrich Co., St. Louis, MO, USA) using a pestle and a mortar at 4°C for 30 min in the presence of 100 mM PMSF (phenylmethane-sulfonyl fluoride, Sigma) prepared in isopropyl alcohol. The mixture was suspended in 50 mM MOPS-NaOH buffer (buffer A) with 10 mM $MgCl_2$ and 1 mM $CoCl_2$ or 1 mM $MnSO_4$ and cell debris was removed by centrifugation at 30,000 × g for 30 min. The chemicals used were purchased from Sigma-Aldrich. The clear supernatant obtained was mixed with 2 ml of the Ni^{2+} nitrilotriacetate (NTA) resin (Qiagen, CA, USA) equilibrated with buffer A. The crude extract–NTA mixture was loaded into a chromatographic column and washed with 20 ml of buffer A. SKGI wild-type and the three mutants were eluted with 200 mM imidazole prepared in buffer A. Purification to homogeneity was achieved by high-performance liquid chromatography (HPLC) using a Shodex Protein WK 802-5 column (8 × 300 mm), pre-equilibrated with buffer A and previously calibrated with the standard marker proteins. Proteins were separated by isocratic elution at a flow rate of 0.5 ml/min with buffer A and detected by a UV–Vis spectrophotometric detector (Knauer) at 280 nm. The pooled fractions, with retention time; $R_t = 12.07$ min, containing glucose isomerase activity was concentrated in centrifugal micro-concentrators (Amicon Inc.,) with a 10-kDa cut-off membrane and stored at –20°C in a glycerol 5% (v/v) solution.

Protein quantification and electrophoresis

Protein concentration was determined using Bradford's method with bovine serum albumin as the standard [8]. The purified enzymes migrated in 10% SDS-polyacrylamide gel electrophoresis under non-reducing conditions, according to the method of Laemmli [24]. Protein bands were visualized by Coomassie brilliant blue staining R-250 (Bio-Rad, USA).

Enzyme assays

The enzyme activity using D-glucose as a substrate was assayed in a reaction mixture containing the enzyme with 50 mM MOPS at the desired pH, 10 mM $MgCl_2$, 1 mM $CoCl_2$ or 1 mM $MnSO_4$ and 15% (w/v) D-glucose, in a volume of 1 ml. Under standard conditions, assays were incubated for 15 min at the desired temperature and then the reaction was stopped by cooling the tubes on ice. Formed fructose was quantified by the cysteine-carbazole sulfuric acid method [13]. One unit of GI activity is defined as the amount of enzyme needed to produce 1 μmol of product per min under the assay conditions.

The enzyme activity using fructose as substrate was assayed in a reaction mixture containing the enzyme (100 μL of an appropriate diluted purified or crude extract) with 50 mM MOPS at the desired pH, 10 mM $MgCl_2$, 1 mM $CoCl_2$ or 1 mM $MnSO_4$ and 15% (w/v) fructose, in a volume of 400 μL. Under standard conditions, assays were incubated for 30 min at optimal temperatures of each enzyme and then the reaction was stopped by cooling the tubes on ice. The amount of glucose generated was determined by the glucose-oxidase (GOD-POD) (Sigma) enzyme system and the OD505 nm was measured after incubating 10 min at 37°C. One unit of glucose isomerase activity is defined as the amount of enzyme needed to produce 1 μmol of product per min under the assay conditions.

Temperature-dependent activity profiles

Temperature-dependent activity profiles were determined at the optimum pH of each enzyme (SKGI and its three derivatives) in buffer A containing 10 mM $MgSO_4$ and 1 mM $CoCl_2$ or 1 mM $MnSO_4$ (for other details, see "Enzyme assays"). The reaction temperatures ranged from 50 to 100°C and the reaction time at each temperature was 30 min.

Thermostability study

The enzyme preparations were incubated at the temperatures of interest in the presence of 50 mM MOPS, 10 mM $MgCl_2$, 1 mM $CoCl_2$, or 1 mM $MnSO_4$ for different periods of time. Samples were withdrawn and stored on ice until the residual activity was determined under the conditions described above.

pH-dependent activity profiles

The effect of pH on the activity of the wild-type and mutated glucose isomerases was investigated in the pH range 5–8 in buffer A containing 10 mM $MgCl_2$ and 1 mM $CoCl_2$ or 1 mM $MnSO_4$ at the optimal temperature of each enzyme.

Kinetic parameters determination

The isomerization of D-glucose was performed in buffer A at the desired pH at 75°C. The substrate concentrations used ranged from 0.1 to 0.9 mM of glucose. The generated reducing sugars were determined at regular time intervals and expressed in equivalent micromoles of glucose per ml of purified enzyme used for the reaction. The V_{max} and km values were calculated from a Lineweaver–Burk plot using the hyper-32 program available at http://www.liv.ac.uk/~jse/software.html.

Metal ion effects

The purified enzymes were incubated overnight at 4°C in buffer A containing 10 mM EDTA, then dialyzed against buffer A containing 2 mM EDTA and finally dialyzed against buffer A. The effect of several metal ions ($CoSO_4$, $ZnSO_4$, $MgSO_4$ $2H_2O$, $FeSO_4$, $MnSO_4$) at 1 mM on the activity of SKGI and its variants, was studied under the optimal conditions of each enzyme. The effect of calcium concentration was investigated by measuring GIs activities in a range of 0–10 mM $CaCl_2$ in presence of 10 mM Mg^{2+} and 1 mM Co^{2+} for SKGI and SKGI F53L and in presence of 10 mM Mg^{2+} and 2.5 mM Mn^{2+} for SKGI G219D and SKGI F53L/G219D. The control activity was defined as the value relative to the activity detected in the absence of ions. The effect of cobalt on the thermostability was studied by incubating the SKGI wild-type and the SKGI F53L/G219D at 85°C for different periods of time in presence of 10 mM Mg^{2+} and with or without 1 mM Co^{2+}.

Amino acid sequence analysis and homology modeling

Sequence analysis and multiple alignments were performed using the program BLAST and CLUSTAL W [1, 34] while the rendering of the alignment, including the superimposition of secondary structures, were conducted using the ESPript utility [18].

The 3D homology model of SKGI was generated using the SWISS-MODEL software (http://www.expasy.org/swissmod/). The molecular modeling of SKGI and its variants were performed using the crystal structure of OLGI (*Streptomyces olivochromogenes* GI) solved to 0.86-Å resolution (PDB accession code 1MUW) with which SKGI possess 95% sequence identity (OLGI accession number P15587) [14]. The PyMOL molecular Graphics System (DeLano Scientific, San Carlos, CA. http://www.pymol.org) and the graphics program TURBO-FRODO [28] were used to visualize and analyze the generated model structure.

Results and discussion

Design of mutations, construction, and purification of mutant enzymes

Previous studies focused on the role of the two catalytic histidines (H54 and H220) in glucose isomerases demonstrating their important role in substrate binding and isomerization [2, 3, 23]. Assuming that the amino acids linked to these histidines could also have an importance in the physico-chemical behavior of the enzyme, the primary structure alignment of SKGI with other glucose isomerases (Fig. 1) was inspected. This alignment indicated that H54 is surrounded by two conserved residues F53 and D55 except for the substitution F53L in the extremely thermostable GIs from the *Thermus* genus. In addition, effects upon stability for small-to-large substitutions, such as L/F, V/A or G/A have previously been described to destabilize the enzyme [19, 25–27]. As opposed hereto, the large-to-small substitutions reducing structural hindrance effects might result in an enhancement of the enzyme thermostability [21]. Thus, with the aim of increasing the thermal stability of SKGI, F53L mutation was performed.

Inspection of the alignment in the H220 region shows that this catalytic residue is preceded by a glycine in all reported GIs from *Streptomyces* species instead of an asparagine in

GIs from *Thermotoga* genus and an alanine in GIs from *Thermus* genus. Besides their higher thermostability, these latter GIs are described to be optimally active at pH ≥7 while SKGI displays its optimal activity at pH 6.5. On the basis of this observation, and in order to study the role of G219 residue on the physico-chemical properties of SKGI, we considered substituting the latter by various amino acids. In this study, we report the effect of the G219D mutant, which displayed very interesting properties matching better with those required for industrial applications.

SKGI and mutant enzymes derivatives F53L, G219D, and F53L/G219D were constructed in an over-expression plasmid (pET-21a) allowing fusion with the His-tag. Then, all of these enzymes were produced and purified as described in the Materials and methods section. Wild-type and mutant proteins exhibited a single protein band on native PAGE corresponding to a protein of nearly 180 kDa. Electrophoresis under denaturing conditions (12% SDS-PAGE) revealed a single band and a molecular mass of about 45 kDa.

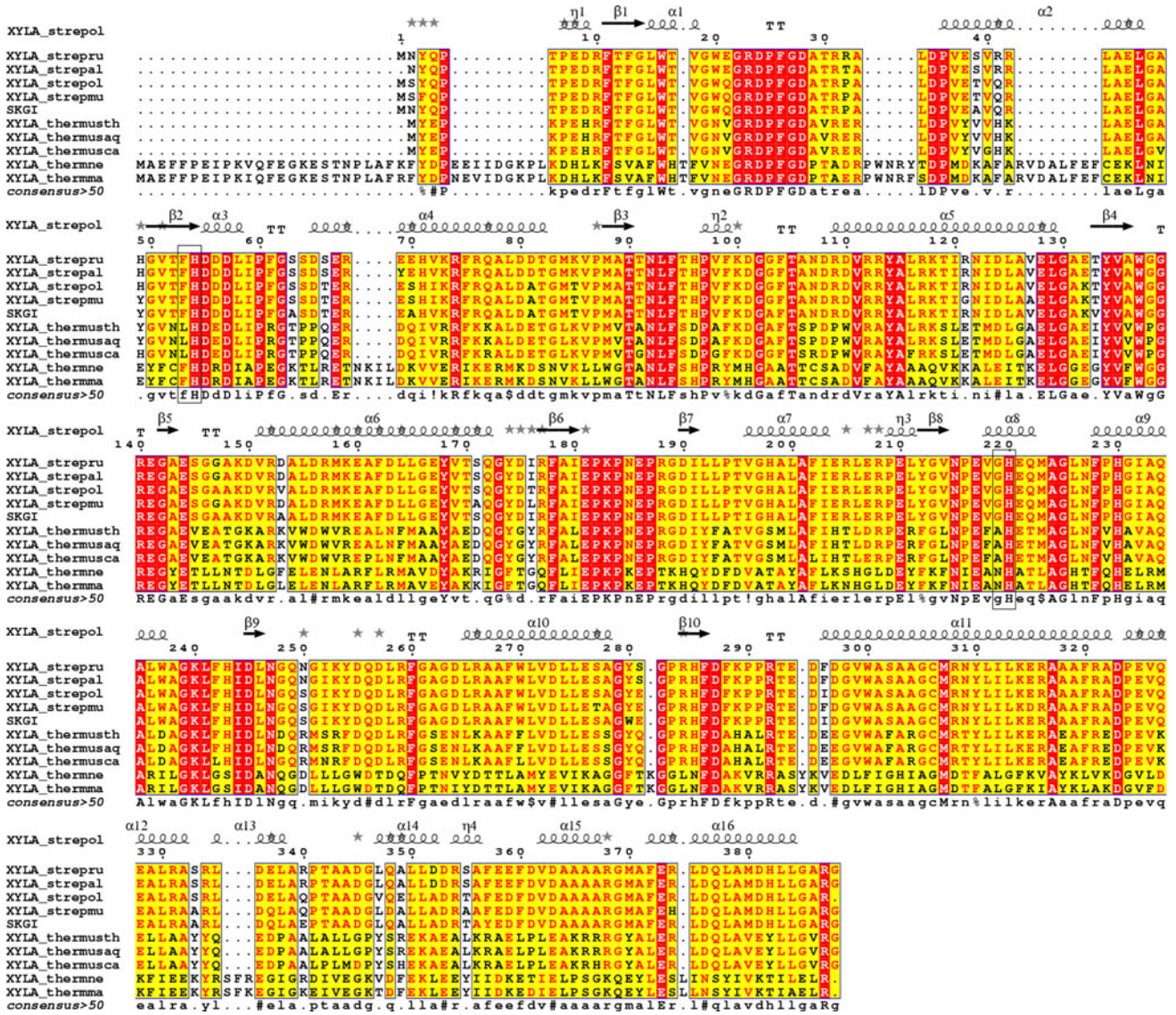

Fig. 1 Structure-based multiple sequence alignment of SKGI in comparison to other glucose isomerases. The secondary structure elements of known glucose isomerase 3D structures are indicated. XYLA_strepol; *Streptomyces olivochromogenes* (accession number P15587, PDBID 1MUW), XYLA_strepru; *S rubiginosus.* (accession number AAA26838), XYLA_strepal; *S. albus* (accession number P24299), XYLA_strepmu; *S. murinus* (accession number P37031), XYLA_thermusth; *Thermus thermophilus* (accession number P26997), XYLA_thermusaq; *Thermus aquaticus* (accession number A39404), XYLA_thermusca; *Thermus caldophilus* (accession number P26997), XYLA-thermone; *Thermotoga neapolitana* (accession number P45687), XYLA-thermoma; *Thermotoga maritima* (accession number NP229467)

Effect of the F53L mutation on enzyme properties

The purified F53L mutant enzyme was found to have a specific activity of 14.6 U/mg, which is approximately 1.6-fold higher than that of the wild-type enzyme.

As expected, the comparative study of physico-chemical properties between SKGI and the generated mutants showed that the mutation F53L increased the thermal stability. As shown in Fig. 2a, thermostability profiles at 85°C indicate a half-life time of 70 min for F53L instead of 50 min for the wild-type enzyme. The physico-chemical characterization showed that this substitution did not have a significant effect on the temperature profile (Fig. 2b) and that the mutated enzyme displayed the same activation behavior toward different metal ions as wild-type SKGI (Table 1), but led to a slight shift in the optimum pH from 6.5 to 7 (Fig. 3). However, it conserved 80% of its activity at pH 6.5, which is approximately 47% higher than that of the wild-type at the same experimental conditions.

To explore the possible role of F53 on the kinetic properties of SKGI, we determined the kinetic constant values on the basis of the Lineweaver–Burk plots (Table 2). This study showed that the F53L mutation mainly increased the catalytic efficiency to 2.54 mM^{-1} min^{-1} instead of 1.99 mM^{-1} min^{-1} for wild-type SKGI, but slightly decreased the glucose binding affinity to the active site since K_m increased from 201 for the SKGI to 258 mM.

These properties revealed the significant role of the phenylalanine residue, linked to the catalytic H54, on the SKGI thermostability and catalytic efficiency and resulted in SKGI F53L being more useful than the wild-type for application in the production of fructose syrup.

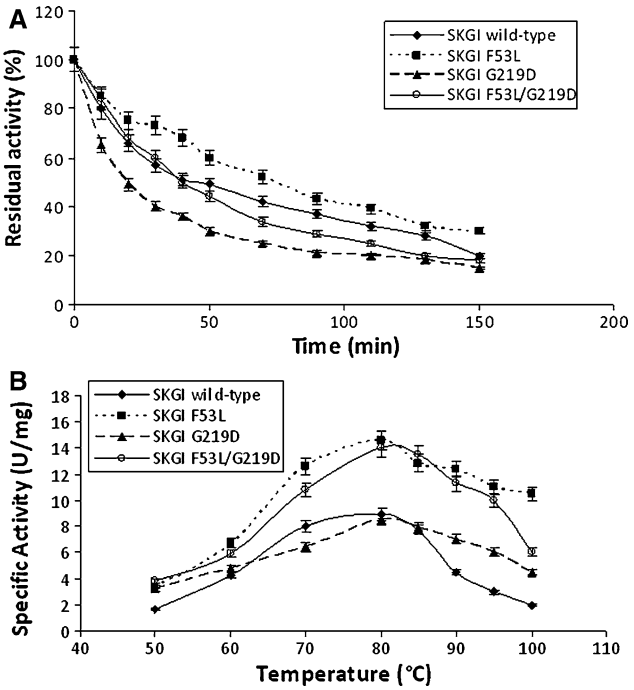

Fig. 2 Temperature effect on SKGI (*filled diamond*), SKGI F53L (*filled square*), SKGI G219D (*filled triangle*) and SKGI F53L/G219D (*open circle*). **a** Thermostability at 85°C. **b** Temperature-dependent activity profiles

Effect of the G219D mutation on enzyme properties

The mutation G219D remarkably decreased the thermostability of SKGI showing a half-life time of only 20 min compared to 50 min for the wild-type at 85°C (Fig. 2a), kept the optimal temperature unchanged (Fig. 2b) and slightly shifted the optimal pH from 6.5 to 7 (Fig. 3).

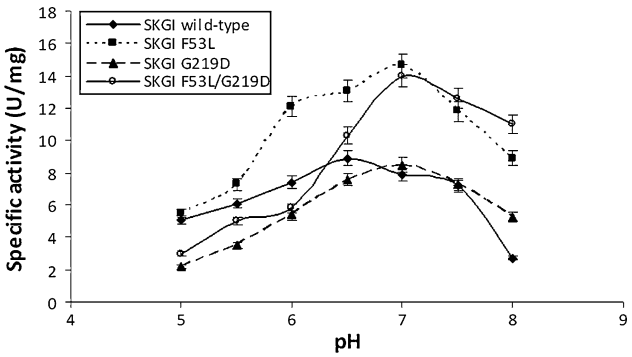

Fig. 3 Effect of pH on the activity of wild-type SKGI (*filled diamond*), SKGI F53L (*filled square*), SKGI G219D (*filled triangle*), and SKGI F53L/G219D (*open circle*)

Table 1 Effect of metal ions at a concentration of 1 mM on the activity of SKGI wild-type, SKGI F53L, SKGI G219D, and SKGI F53L/G219D enzymes. The control is defined as the value relative to the activity detected in the absence of ions

	Relative activities (%)					
	Control	Mn^{2+}	Zn^{2+}	Fe^{2+}	Co^{2+}	Mg^{2+}
SKGI wild-type	60	64	16	35	83	100
SKGI F53L	60	70	20	40	80	100
SKGI G219D	0	100	0	20	10	72
SKGI G219D/F53L	20	100	50	15	63	86

Table 2 Kinetic parameters of SKGI wild-type and mutated enzymes toward glucose

	V_m (U/mg)	K_m (mM)	k_{cat} (min^{-1})	k_{cat}/K_m (mM^{-1} min^{-1})
SKGI wild-type	8.9 ± 0.6	201 ± 15.5	400	1.99
SKGI F53L	14.6 ± 0.8	258 ± 18.2	657	2.54
SKGI G219D	8.54 ± 0.4	247 ± 11.7	388	1.57
SKGI G219D/F53L	13.6 ± 0.3	252 ± 16.9	612	2.42

The study of the kinetic parameters of the SKGI G219D mutant showed that this mutation slightly lowered the glucose binding affinity for the catalytic site compared to the wild-type enzyme and consequently faintly decreased the catalytic efficiency (k_{cat}/K_m) from 1.99 to 1.57 mM^{-1} min^{-1} (Table 2).

Interestingly, the study of the metal ions effect showed that the G219D mutant was not inhibited by calcium ions. In fact, it kept 91 and 80% of its optimal activity when supplemented with 2.5 and 10 mM Ca^{2+} instead of only 50 and 10% for the wild-type, respectively (Fig. 4). In addition, the study of other metal ions effects showed that the mutant G219D was strongly activated by Mn^{2+} ions but only partially activated by Mg^{2+} and Co^{2+} ions and was independent towards the latter for its thermostability (Table 1). We have also demonstrated that the optimal activity for this mutant was obtained with 10 mM Mg^{2+} and 1 mM Mn^{2+} unlike the wild-type, which was activated with 10 mM Mg^{2+} and 1 mM Co^{2+}. These results suggest that the aspartic acid substituting G219 affected the metal binding site of cobalt preventing its binding, but also that of the inhibitor calcium ion.

Hence, mutant G219D possesses a very interesting behavior towards metal ions, though it is less thermostable and showed a lower catalytic efficiency than the wild-type. With the aim of overcoming this problem, we constructed the double mutant F53L/G219D.

Effect of the F53L/G219D double mutation on enzyme properties

As expected, the double mutation improved the thermal stability as compared to the G219D single mutation, displaying a residual activity of 44% instead of 49% for SKGI after 50 min at 85°C (Fig. 2a). The catalytic efficiency of F53L/G219D (Table 2) was also improved to 2.42 mM^{-1} min^{-1} compared to the G219D mutant (1.57 mM^{-1} min^{-1}) and to the wild-type enzyme (1.99 mM^{-1} min^{-1}), while slightly decreased compared to the F53L mutant (2.54 mM^{-1} min^{-1}).

Remarkably, the study of the metal ion effect on the double mutant activity showed the same behavior as that of the G219D mutant. Indeed, the double mutant kept 87% of its optimal activity in 2.5 mM Ca^{2+} whilst the G219D mutant kept 91% of its activity under the same conditions (Fig. 4) against 50% for the wild-type enzyme. These results are highly interesting, since no previous reports on GIs displaying such resistance to calcium inhibition exist to the best of our knowledge.

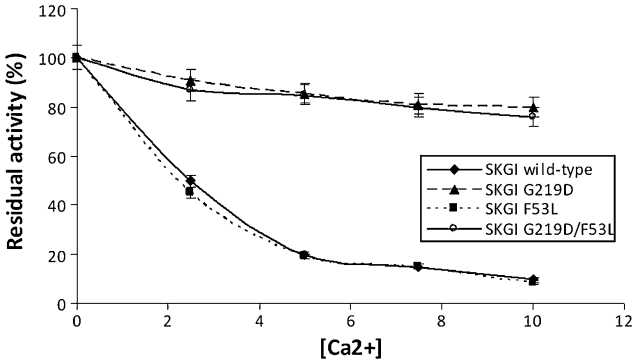

Fig. 4 Effect of calcium ions on the activity of SKGI (*filled diamond*), SKGI F53L (*filled square*), SKGI G219D (*filled triangle*), and SKGI F53L/G219D (*open circle*) in the presence of 10 mM Mg^{2+} and 1 mM Co^{2+} for SKGI and SKGI F53L and in the presence of 10 mM Mg^{2+} and 2.5 mM Mn^{2+} for SKGI G219D and SKGI F53L/G219D

The double mutant is moreover characterized by being cobalt ion independent for its thermal stability supporting further its usefulness in HFCS production process (Fig. 5).

Structural interpretation

Analysis of the SKGI model indicated that the F53 residue is located in the C-terminal end of the β2 sheet containing the key active site residue H54. Careful inspection of the F53 suggests that it is implicated in interactions between the β2 sheet and the α3 helix principally by hydrophobic interaction with the L129 (Fig. 6a). As shown by the model in Fig. 6b, substitution of F53 by a leucine could lead to a change in the orientation of the side chain and slightly twist the β2 sheet, and thereby create a new hydrophobic interaction between the L58 and L53 stabilizing the catalytic residue H54. This could explain the observed improvement of the catalytic efficiency and the thermostability of F53L and F53L/G219D mutants. New hydrophobic contacts might also appear between L53 and F75 located in the α2 helix thus exerting a stabilizing effect. This observation is

reinforced by the fact that the α2 helix is situated at the surface of the protein unlike the α3 helix and exposed to the solvent, disregarding whether being on a monomeric or a tetrameric form. This may contribute to increasing the thermostability of F53L, which is in accordance with the findings that stabilizing structures at the surface of the protein contribute to improvements of thermal stabilities [7, 9].

Residue G219 is located at the catalytic site of the protein. According to the SKGI G219D model, D219 could establish a new hydrogen bond with N247, and thereby create a barrier reducing the accessibility of a large ion such as Ca^{2+} to the metal site and consequently reducing its inhibitory effect on SKGI activity (Fig. 6d). As opposed hereto, a smaller ion such as Mn^{2+} would probably be able to enter the site and activate the enzyme.

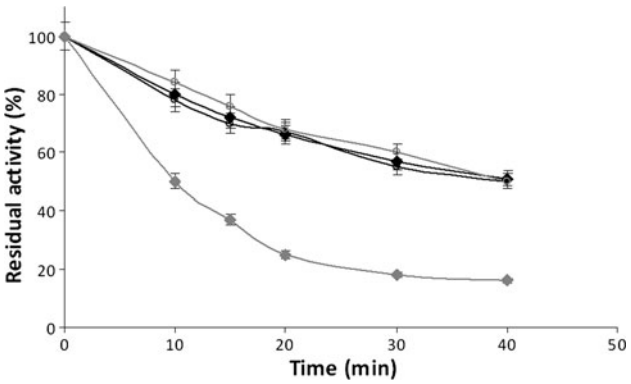

Fig. 5 Thermal stability at 85°C of wild-type SKGI (*filled diamond*) and SKGI F53L/G219D (*open circle*) in the presence of 10 mM Mg^{2+}; with 1 mM Co^{2+} (in *black*) or without Co^{2+} (in *grey*)

The implication of the catalytic metal binding site on the inhibitory effect of calcium ion was investigated by Fuxreiter et al. [15] and by Gerczei et al. [16]. The authors specifically engineered the D254E/D256E double mutation to reduce the space available for binding and consequently reduce the inhibitory effect of Ca^{2+} in the xylose isomerase from *Arthrobacter* B3728. They found, in agreement with our results, that the spatial reduction in site 2 might reduce the inhibitory effect of Ca^{2+} ions. However, the decrease in Ca^{2+} inhibition was accompanied by an important reduction in the enzymatic activity, whereas for the G219D mutant reported herein the enzymatic activity was only very slightly decreased compared to the wild-type. This could be explained by the fact that the G219 is not directly implicated in the ion binding while the two aspartate residues 254 and 256 are involved in maintaining the metal during the isomerization reaction [3].

As shown by the SKGI and SKGI G219D model in Fig. 6c, d, respectively, the Gly/Asp substitution leads to the introduction of a big side chain in a very flexible region between the two catalytic residues H220 and E217

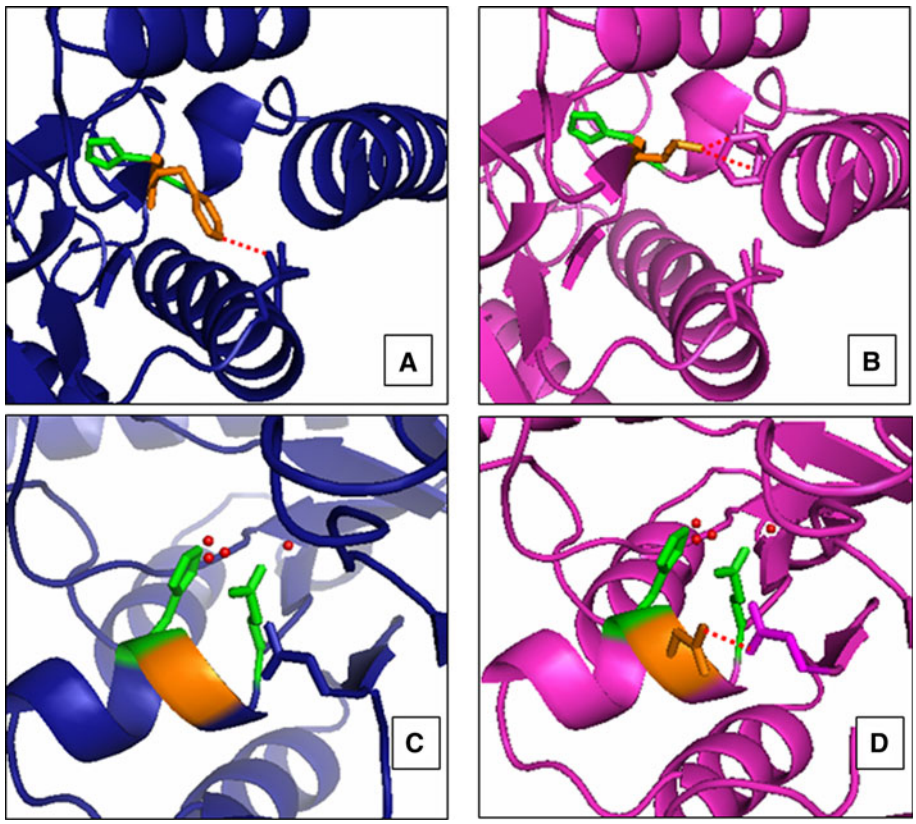

Fig. 6 Close-up views showing the active sites in SKGI, SKGI F53L, and SKGI G219D homology models. **a**, **c** Respective positions of F53 and G219 residues in SKGI model. **b** Position of L53 in SKGI F53L model. **d** Position of D219 in SKGI G219D model. The mutated residues and the catalytic amino acids H54 and H220 are shown in *sticks*. Hydrogen bonds and hydrophobic interactions are indicated as *stippled lines*. Metal ion binding sites are indicated as *spheres*

implicated in the M2 ion binding site [3]. This might result in a reduction of the flexibility of this region and thereby disturb the ion binding and consequently reduce the thermostability and the catalytic efficiency of the SKGI G219D variants [4].

Conclusions

Using a combined site-directed mutagenesis, sequence alignment, and molecular modeling approach, we generated a set of very attractive SKGI derivatives, in particular mutant F53L/G219D, being potentially useful for application in the HFCS production process. This enzyme is more efficient than the wild-type SKGI, since it is resistant to Ca^{2+} inhibition and independent of Co^{2+} ions for its thermal stability. The double mutant illustrates the combined effect of the F53L mutation, which increases the specific activity and the thermal stability and the G219D mutation, which allowed the resistance to calcium inhibition and cobalt independency. These findings highlighted the importance of residues linked to the catalytic residues H54 and H220 in SKGI. According to our modeling studies, the thermal stability improvement might be due to the formation of new hydrophobic interactions stabilizing the protein surface, whereas the resistance to calcium inhibition was due to a narrowing of the binding site of the catalytic ion.

Acknowledgments All authors have agreed to submit this manuscript to the Journal of Industrial Microbiology and Biotechnology. This work was funded by the Tunisian Ministry of Higher Education, the French-Tunisian CMCU programme no. 09G 0801 and the French National Research Center (CNRS).

References

1. Altschul SF, Madden TL, Schaffer AA, Zhang J, Zhang Z, Miller W, Lipman DJ (1997) Gapped BLAST and PSI-BLAST: a new generation of protein database search programs. Nucleic Acids Res 25:3389–3402
2. Batt CA, Jamieson AC, Vandeyar MA (1990) Identification of essential histidine residues in the active site of *Escherichia coli* xylose (glucose) isomerase. Proc Natl Acad Sci USA 87:618–622
3. Bennett BC, Yeager M (2010) The lighter side of a sweet reaction. Structure 18:657–659
4. Bhosale SH, Rao MB, Deshpande VV (1996) Molecular and industrial aspects of glucose isomerase. Microbiol Rev 60: 280–300
5. Borgi MA, Srih-Belguith K, Ben Ali M, Mezghani M, Tranier M, Haser R, Bejar S (2004) Glucose isomerase of the *Streptomyces* sp. SK strain: purification, sequence analysis and implication of alanine 103 residue on the enzyme thermostability and acidotolerance. Biochimie 86:561–568
6. Borgi MA, Rhimi M, Bejar S (2007) Involvement of alanine 103 residue in kinetic and physicochemical properties of glucose isomerases from *Streptomyces* species. Biotechnol J 2:1–6
7. Borgi MA, Rhimi M, Aghajari N, Ben Ali M, Juy M, Haser R, Bejar S (2009) Involvement of cysteine 306 and alanine 63 in the thermostability and oligomeric organization of glucose isomerase from *Streptomyces* sp. SK. Biologia 64:845–851
8. Bradford MM (1976) A rapid and sensitive method for the quantification of microgram quantities of protein utilizing the principal of protein-dye binding. Anal Biochem 72:248–254
9. Chang C, Park BC, Lee D, Suh SW (1999) Crystal structures of thermostable xylose isomerases from *Thermus caldophilus* and *Thermus thermophilus*: possible structural determinants of thermostability. J Mol Biol 288:623–634
10. Chauthaiwale JV, Rao MB (1994) Production and purification of extracellular D-xylose isomerase from an alkaliphilic, thermophilic *Bacillus* sp. Appl Environ Microb 60:4495–4499
11. Cotter WP, Lloyd NE, Hinman CW (1971) Method for isomerizing glucose syrups. US Patent 3,623,953
12. De Boeck M, Kirsch-Volders M, Lison D (2003) Cobalt and antimony: genotoxicity and carcinogenicity. Mutat Res 533:135–152
13. Dische Z, Borenfreund E (1951) A new spectrophotometric method for the detection and determination of keto sugars and trioses. J Biol Chem 192:583–587
14. Fenn TD, Ringe D, Petsko GA (2004) Xylose isomerase in substrate and inhibitor Michaelis states: atomic resolution studies of a metal-mediated hydride shift. Biochemistry 43:6464–6474
15. Fuxreiter M, Böcskei Z, Szeibert A, Szabó E, Dallmann G, Naray-Szabo G, Asboth B (1997) Role of electrostatics at the catalytic metal binding site in xylose isomerase action: Ca (2+)-inhibition and metal competence in the double mutant D254E/D256E. Proteins 28:183–193
16. Gerczei T, Böcskei Z, Szabó E, Asboth B, Naray-Szabo G (1999) Structure determination and refinement of the Al3+ complex of the D254, 256E mutant of Arthrobacter D-xylose isomerase at 2.40 A0, resolution. Further evidence for inhibitor-induced metal ion movement. Int J Biol Macromol 25:329–336
17. Goldstein WE (1990) Enzymes in starch processing and baking. In: Gerhartz W (ed) Enzymes in industry. VCH Publishers, New York, pp 92–102
18. Gouet P, Robert X, Courcelle E (2003) ESPript E./ENDscript: Extracting and rendering sequence and 3D information from atomic structures of proteins. Nucleic Acids Res 31:3320–3323
19. Hurley JH, Baase WA, Matthews BW (1992) Design and structural of alternative hydrophobic core packing arrangements in bacteriophage T4 lysozyme. J Mol Biol 224:1143–1159
20. Khemakhem B, Ben Ali M, Aghajari N, Juy M, Haser R, Bejar S (2008) Engineering of the α-amylase from *Geobacillus stearothermophilus* US100 for detergent incorporation. Biotechnol Bioeng 102:380–389
21. Kim M, Weaver JD, Lei XG (2008) Assembly of mutations for improving thermostability of *Escherichia coli* AppA2 phytase. Appl Microbiol Biotechnol 79:751–758
22. Kobayashi M, Shimizu S (1999) Cobalt protein. Eur J Biochem 261:1–9
23. Kovalevsky AY, Hanson L, Fisher SZ, Mustyakimov M, Mason SA, Forsyth VT, Blakeley MP, Keen DA, Wagner T, Carrell HL, Katz AK, Glusker JP, Langan P (2010) Metal ion roles and the movement of hydrogen during reaction catalyzed by D-xylose isomerase: a joint X-Ray and neutron diffraction study. Structure 18:688–699
24. Laemmli UK (1970) Cleavage of structural proteins during the assembly of the head of bacteriophage T4. Nature 227:680–685
25. Lim WA, Farruggio DC, Sauer RT (1992) Structural and energetic consequences of disruptive mutations in a protein core. Biochemistry 31:4324–4333
26. Lim WA, Hodel A, Sauer RT, Richards FM (1994) The crystal structure of a mutant protein with altered but improved hydrophobic core packing. Proc Nat Acad Sci USA 91:423–427

27. Liu R, Baase WA, Matthews BW (2000) The introduction of strain and its effects on the structure and stability of T4 lysozyme. J Mol Biol 295:127–145
28. Roussel A, Cambillau C (1992) TURBO-FRODO, biographics. AFMB, Marseille
29. Sambrook J, Fritsh EF, Maniatis T (1989) Molecular cloning: a laboratory manual, 2nd edn. Cold Spring Harbor Laboratory Press, NY, pp 23–38
30. Sanchez S, Smiley KL (1975) Properties of D-xylose isomerase from Streptomyces albus. Appl Microbiol 29:745–750
31. Shaw A, Bott R, Day AG (1999) Protein engineering of α-amylase for low pH performance. Curr Opin Biotechnol 10:349–352
32. Somers E (1974) The toxic potential of trace metals in foods. J Food Sci 39:215–217
33. Srih-Belghith K, Bejar S (1998) A thermostable glucose isomerase having a relatively low optimum pH: study of activity and molecular cloning of the corresponding gene. Biotechnol Lett 20:553–556
34. Thompson JD, Higgins DG, Gibson TJ (1994) CLUSTAL W: improving the sensitivity of progressive multiple sequence alignment through sequence weighting, position-specific gap penalties and weight matrix choice. Nucleic Acids Res 22:4673–4680
35. Vieille C, Epting KL, Kelly RM, Zeikus JG (2001) Bivalent cations and amino-acid composition contribute to the thermostability of *Bacillus licheniformis* xylose isomerase. Eur J Biochem 268:6291–6301